Absolute Rate Constants for the Reaction of OH with NO_2 in N_2 and He from 225 to 389 K

Larry G. Anderson

Environmental Science Department, General Motors Research Laboratories, Warren, Michigan 48090 *(Received: June 22, 1979; In Final Form: April 23, 1980)*

The temperature dependence of the rate of the reaction $OH + NO_2 + N_2 \rightarrow HNO_3 + N_2$ was investigated by using a discharge flow system for OH production and resonance fluorescence for its detection. The reaction was investigated at room temperature in He, and between 225 and 389 K in N_2. The temperature dependence could be fit by the Arrhenius expression $(1.6 \pm 0.4) \times 10^{-31} \exp[(1560 \pm 270)/1.987T]$ cm^6 molecule^{-2} s^{-1} or preferably by $(2.3 \pm 0.6) \times 10^{-30}(T/298)^{-2.9}$ cm^6 molecule^{-2} s^{-1}. Earlier data have been used to determine the temperature dependence of the high-pressure limiting rate constant for this reaction. Troe's simplified expression for calculating rate constants in the falloff region was used to compare the appropriateness of different limiting values for the description of the experimentally observed pressure dependence of the rate constant. This reevaluation of the rate data suggests more appropriate values for k_0 and k_∞ for use in atmospheric modeling: $k_0 = 2.3 \times 10^{-30}(T/298)^{-2.9}$ cm^6 molecule^{-2} s^{-1} and $k_\infty = 1.2 \times 10^{-11}(T/298)^{-1.6}$ cm^3 molecule^{-1} s^{-1}.

Introduction

The atmospheric importance of the reaction

$$OH + NO_2 + N_2 \rightarrow HNO_3 + N_2 \qquad (1)$$

has been recognized for several years.[1] In the stratosphere, this reaction simultaneously removes reactive HO_x and NO_x species of importance in ozone-destruction cycles. In the troposphere, this reaction is the most important gas-phase removal process for NO_2. Recent tropospheric modeling has shown that photochemically generated ozone is very sensitive to the rate constant used for this reaction, since it converts the photochemically active NO_2 to a less active form, HNO_3.[2,3] In the urban atmosphere, reaction 1 is expected to be the dominant removal process for active NO_x species.[4]

Reaction 1 has been directly investigated at high pressures by using flash photolysis techniques[5-9] and at low pressures by using discharge-flow systems.[10-15] High-pressure studies have provided information about the temperature and pressure dependence of this reaction in the falloff region between second-order and third-order behavior. The third-order behavior of the reaction is described most directly by the low pressure studies. Due to the importance of this reaction in the atmosphere, its temperature dependence should be studied in N_2. This work reports the first direct measurement of the temperature dependence of the termolecular rate constant for the reaction in N_2 between 225 and 389 K, as well as a room temperature measurement in He. Falloff curves are calculated from the results obtained and are tested by comparison with experimental data for the reaction over a broad range of temperatures and pressures.

Experimental Section

The apparatus is a conventional fast-flow system consisting of a Pyrex flow tube 2.5 cm in diameter, with a temperature controlled length of about 70 cm. The downstream end of the flow tube is connected to a fluorescence cell, which is illuminated by a collimated beam of resonance radiation from the $A\ ^2\Sigma \rightarrow X\ ^2\Pi$ (0,0) band of OH. Resonantly scattered photons are detected by a filtered photomultiplier, which is orthogonal to both the gas flow and the direction of illumination.

Hydroxyl radicals are produced in the flow system by passing a mixture of hydrogen in helium through a microwave discharge, forming hydrogen atoms. The H atoms are then allowed to react with NO_2 (Matheson, 99.5% pure) added downstream of the discharge through a fixed injector or a multiholed 0.6-cm diameter movable Pyrex injector, which is concentric with the main flow tube. The helium or nitrogen carrier gas was added to the flow downstream of the microwave discharge.

The reaction of H atoms with NO_2 has been shown to produce vibrationally excited OH in $v = 1$, $v = 2$, and a small amount in $v = 3$.[16-18] Spencer and Glass[18] have investigated the rates of vibrational deactivation of $v = 1$ and $v = 2$ by H and NO. In their analysis, they assumed that the vibrational deactivation efficiency of NO_2 is about 1/4 that of H atoms. This gives a vibrational deactivation rate constant of about 7.5×10^{-11} cm^3 molecule^{-1} s^{-1}, which at the lowest NO_2 concentration used of about 1×10^{14} molecule cm^{-3} gives a lifetime for vibrationally excited OH of about 0.13 ms. This is without considering the additional deactivation by N_2 which is at least two orders of magnitude more concentrated than NO_2. A negligible amount of vibrationally excited OH could persist to the minimum OH observation time of about 2 ms. If vibrationally excited OH had a significant effect on this study of the OH reaction with NO_2, curvature in the pseudo first-order decay plots would be observed. No such curvature was observed.

The hydrogen/helium, helium, and nitrogen flows were controlled by using calibrated mass flow controllers (Tylan). The NO_2 was taken from a cylinder of liquid N_2O_4 through a mass flow meter (Hastings) and a needle valve, which were maintained at a constant temperature. The mass flow meter response was calibrated by measuring the pressure rise in a calibrated volume. This pressure rise was corrected for NO_2 dimerization. The pressure in the flow system was measured with a capacitance manometer (MKS) and the temperature was measured with a thermocouple located inside the movable injector. The temperature in the flow system was maintained constant by the circulation of a heated or cooled fluid through the jacket of the flow tube. A 30 L/s rotary pump (Leybold-Heraeus) was used to maintain velocities between 1.4×10^3 and 3.3×10^3 cm s^{-1} at pressures between 0.8 and 2.8 torr (1 torr = 133.32 Pa). The OH radical wall loss rate was minimized by coating the flow tube with hot, syrupy phosphoric acid.

0022-3654/80/2084-2152$01.00/0

TABLE I: Summary of Experimental Conditions and Rate Constants for the OH + NO_2 + M Reaction[a]

T, K	no. of expermt	$10^{-14}(NO_2)$, molecule cm^{-3}	M	press., torr	k_w, s^{-1}	$10^{30}k_0$, cm^6 molecule^{-2} s^{-1}
298	12	1.65-13.96	He	1.49	49 ± 2	1.6 ± 0.1
298	10	2.88-12.40	He	2.70	27 ± 8	1.9 ± 0.1
298			He			av 1.7 ± 0.2
225	10	2.22-4.81	N_2	1.10	70 ± 6	3.6 ± 0.4
229	11	2.06-4.30	N_2	0.97	78 ± 6	5.2 ± 0.4
234	10	2.99-5.26	N_2	1.21	67 ± 22	5.4 ± 1.3
229			N_2			av 4.7 ± 1.4
263	10	3.21-10.54	N_2	0.99	65 ± 6	2.9 ± 0.3
263	10	3.06-7.31	N_2	1.17	70 ± 4	2.1 ± 0.2
263	10	2.24-6.40	N_2	1.47	62 ± 6	2.6 ± 0.2
263	10	1.81-3.95	N_2	1.78	54 ± 10	2.8 ± 0.6
263			N_2			av 2.6 ± 0.7
298	12	1.21-10.49	N_2	0.84	42 ± 4	2.5 ± 0.2
298	10	1.61-11.01	N_2	1.23	22 ± 2	2.8 ± 0.1
298	11	1.63-6.16	N_2	1.57	44 ± 4	2.8 ± 0.2
298	10	1.48-6.06	N_2	1.70	15 ± 3	2.3 ± 0.1
298	10	1.13-5.87	N_2	1.92	24 ± 2	2.2 ± 0.1
298			N_2			av 2.5 ± 0.4
351	10	3.76-12.86	N_2	1.19	61 ± 3	1.5 ± 0.1
351	10	4.49-16.25	N_2	1.48	56 ± 4	1.5 ± 0.1
351	10	5.72-10.07	N_2	1.87	67 ± 5	1.5 ± 0.2
351			N_2			av 1.5 ± 0.2
389	10	9.52-18.01	N_2	1.25	67 ± 6	0.7 ± 0.1
389	8	11.37-27.76	N_2	1.50	50 ± 11	1.0 ± 0.2
389	10	7.92-27.35	N_2	1.80	49 ± 4	1.0 ± 0.1
389	10	4.35-16.76	N_2	1.98	27 ± 5	1.1 ± 0.1
389	10	2.39-9.20	N_2	2.32	29 ± 3	0.9 ± 0.1
389			N_2			av 1.0 ± 0.3

[a] Uncertainty limits are ±σ determined from a weighted-least-squares fit of the pseudo-first-order rate constant vs. concentration data.

Results

The initial OH concentration was about 10^{12} cm^{-3}. At these low concentrations radical–radical reactions, such as

$$OH + OH \rightarrow H_2O + O \quad (2)$$

will be of negligible importance in comparison to the wall loss rate of about 50 s^{-1}. The reaction of OH with NO_2 was studied for NO_2 concentrations between about 1×10^{14} and 28×10^{14} molecule cm^{-3}, and third-body (He and N_2) concentrations between about 3×10^{16} and 9×10^{16} molecule cm^{-3}.

The wall loss rate, k_w, for OH was determined by introducing a small flow of NO_2 through the movable injector into the flow of hydrogen atoms in diluent. The OH fluorescence signal was monitored as a function of reaction distance, and k_w was determined from a fit to a first-order decay of OH vs. time. The effective bimolecular rate constant for the OH reaction 1 at a particular pressure was given by the slope of a plot of the observed pseudo-first-order rate constant vs. NO_2 concentration. The wall loss rate for OH given by the intercept of such plots was regularly compared with the more direct determination of k_w. These values were generally found to compare within 10%. The wall loss rates determined from the intercepts of the plots are presented in Table I. These values were found to be relatively constant during the course of a day of experimentation.

Westenberg and de Haas[11] and Anderson et al.[12] have reported a nonzero intercept in plots of the effective bimolecular rate constant vs. total pressure, which was interpreted as a heterogeneous removal process. Due to the limited pressure range of our experiments, the importance of heterogeneous removal processes could not be accurately evaluated. However, such plots for our data gave zero intercepts within the experimental uncertainty, hence heterogeneous removal was neglected. The more recent investigations of reaction 1 in discharge-flow systems have not reported the heterogeneous removal of OH.[13-15]

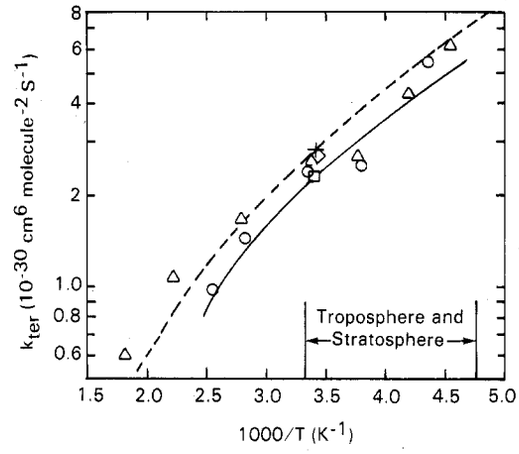

Figure 1. Arrhenius plot of k_0 vs. $1000/T(K^{-1})$: (△) Anastasi and Smith (extrapolated to low pressure);[7] (□) Anderson et al.;[12] (◇) Harris and Wayne;[14] (+) Howard and Evenson;[13] (○) this work. The solid line represents a fit to the data from this work to the equation $k_0 = 2.3 \times 10^{-30}(T/298)^{-2.9}$. The dashed line represents the results of a recent evaluation of kinetics data for this reaction.[19]

The investigation of the temperature dependence of the reaction in N_2 was complicated by the nonnegligible dimerization of NO_2 at subambient temperatures. The rate of NO_2–N_2O_4 equilibration was calculated for the movable injector and flow tube at the lower temperatures. This resulted in a reduction in NO_2 flow of 20% near 229 K, 14% near 263 K, and less than 1% at 298 K. It was assumed that reaction of OH with N_2O_4 occurred at a negligible rate.

Table I summarizes the results of 224 experiments investigating the OH reaction with NO_2 in He and N_2. Tables listing the experimental conditions employed in the measurement of each pseudo-first-order rate constant are available as supplementary material. Figure 1 shows an Arrhenius plot of the termolecular rate constants. The Arrhenius fit of this data resulted in $k_0 = (1.6 \pm 0.4) \times 10^{-31}$

TABLE II: Comparison of the Direct Measurements of the Rate of the Termolecular Reaction OH + NO_2 + M

ref	technique[a]	third body	press., torr	$10^{30}k_0$ (at 298 K), cm^6 molecule^{-2} s^{-1}	temp dependence
5	FP-RA	He	20-300	1.1	
10	DF-RF	Ar	0.5-10	1.0	
		N_2	8	2.0	
11	DF-ESR	He	0.5-5	1.6	−2200 cal/mol
		Ar	0.5-4	0.8	
12	DF-RF	He	1-10	1.0	
		Ar	1-10	1.0	−1800 cal/mol, $T^{-2.5}$
		N_2	1-8	2.3	
13	DF-LMR	N_2	0.5-2	2.9	
14	DF-RF	Ar	1-3	1.5	
		N_2		2.6	
6	FP-RA	N_2	10-120	2.3	
7	FP-RA	He	25	0.9	
		Ar	25	1.1	
		N_2	10-500	2.6	−1600 cal/mol, $T^{-2.6}$
		O_2	25	1.8	
		SF_6	25-500	6.7	
8	FP-RF	Ar	25-650	1.0	
		N_2	25		
15	DF-RF	He	3-9	1.0	−1700 cal/mol, $T^{-2.9}$
		CO_2	4	4.0	
9	FP-RF	He	14-690	*b*	
		Ar	14-840	*b*	
		N_2	14-230	*b*	
		SF_6	14-690	*b*	
this work	DF-RF	He	1.5-3	1.7	
		N_2	0.8-2	2.5	−1600 cal/mol, $T^{-2.9}$

[a] OH production: DF, discharge flow; FP, flash photolysis. OH detection: RA, resonance absorption; RF, resonance fluorescence; ESR, electron spin resonance; LMR, laser magnetic resonance. [b] Wine et al.[9] did not report a value of k_0 from their data.

$\exp[(1560 \pm 270)/1.987T]$ cm^6 molecule^{-2} s^{-1}. The data were also fit to the form $k_0 = (2.3 \pm 0.6) \times 10^{-30}(T/298)^{-2.9}$ cm^6 molecule^{-2} s^{-1}. This preferred fit to the data is shown as the solid line in Figure 1. The room temperature rate constant found in He was $(1.7 \pm 0.5) \times 10^{-30}$ cm^6 molecule^{-2} s^{-1}. The possible contributions to systematic errors have been analyzed and led to an overall error estimate of about ±25%. The error limits reported in this work reflect this overall error estimate.

Discussion

Table II summarizes the published data on the direct measurement of the rate of reaction 1. Our value for the rate of reaction in helium is somewhat higher than most of the results reported previously, but is still in reasonable agreement with those studies. The helium results are based on a limited number of experiments and are subject to greater uncertainty than our nitrogen results. The room temperature result for the nitrogen experiments is in excellent agreement with previously reported results. This work provides the first direct measurement of the temperature dependence of the termolecular reaction in nitrogen over a temperature range from 225 to 389 K. The resulting temperature dependence is in excellent agreement with previous measurements in helium and argon. Figure 1 shows the comparison of the temperature-dependent data for the reaction in nitrogen. There is reasonable agreement with other low-pressure measurements made in nitrogen near room temperature and with the results of extrapolation of high-pressure measurements to the low-pressure regime. The differences seem to be greater at higher temperatures, which are of less interest in the atmosphere. The solid curve in Figure 1 is the result of a least-squares fit to an equation of the form $k_0 = B \cdot (T/298)^{-n}$ for the the rate constants measured in this work. The dashed curve (Figure 1) shows the results of a recent evaluation of low-pressure kinetics data for the OH + NO_2 + N_2 reaction.[19]

Under pressure conditions of the troposphere and stratosphere, where reaction 1 is believed to be of significance, the reaction will be in the falloff region, neither a bimolecular nor a termolecular reaction. Troe[20,21] has developed a simple expression for the calculation of rate constants in the falloff region. The expression is

$$k = \frac{k_0[\mathrm{M}]}{1 + k_0[\mathrm{M}]/k_\infty} 0.8^{\{1+[\log(k_0[\mathrm{M}]/k_\infty)]^2\}^{-1}} \quad (3)$$

where k_0 is the low-pressure limiting rate constant and k_∞ is the high-pressure limiting rate constant. The value of k_0 has been determined in this work. Anastasi and Smith[7] have extrapolated falloff curves for their pressure-dependent data for the rate of reaction 1 to the high-pressure limit. This data gives $k_\infty = 1.3 \times 10^{-11}(T/298)^{-2.0}$ cm^3 molecule^{-1} s^{-1} for the temperature range from 220 to 550 K. Glanzer and Troe[22] have investigated the reverse reaction, nitric acid decomposition in shock tube studies between 900 and 1100 K. Combining the high-pressure limit of the rate data for the decomposition reaction with the equilibrium constant for the reaction, one can determine the high-pressure limit for the recombination reaction 1. In conjunction with the data of Anastasi and Smith[7], the high-pressure limit becomes $k_\infty = 1.2 \times 10^{-11}(T/298)^{-1.6}$ cm^3 molecule^{-1} s^{-1} over the temperature range from 220 to 1100 K.

Troe's expression (3)[20,21] relating the rate constant of a reaction in the falloff region to k_0 and k_∞ has been used to evaluate the fit of falloff curves for different k_0 and k_∞ values to the measured data for the OH reaction with NO_2 in N_2. Three sets of k_0 and k_∞ values were evaluated: (a) $k_0 = 2.3 \times 10^{-30}(T/298)^{-2.9}$ cm^6 molecule^{-2} s^{-1}, this work, and $k_\infty = 1.3 \times 10^{-11}(T/298)^{-2.0}$ cm^3 molecule^{-1} s^{-1}, Anastasi and Smith;[7] (b) $k_0 = 2.3 \times 10^{-30}(T/298)^{-2.9}$ cm^6 molecule^{-2} s^{-1}, this work, and $k_\infty = 1.2 \times 10^{-11}(T/298)^{-1.6}$ cm^3 molecule^{-1} s^{-1}, reevaluated in this work; and (c) $k_0 = 2.6 \times 10^{-30}(T/300)^{-2.9}$ cm^6 molecule^{-2} s^{-1}, NASA evaluation,[19] and

TABLE III: Percentages of Experimentally Determined Rate Constants for OH + NO_2 + N_2 Predicted by Eq 3 with Three Sets of Values for k_0 and k_∞[a]

ref	I, K	(a), %	(b), %	(c), %
High Pressure Data				
7	220	93	86	118
	238	111	106	139
	265	119	114	150
	296	93	90	126
	358	96	96	134
	450	137	141	203
	550	130	138	199
av		111	110	153
8	298	114	112	141
9	247	99	94	128
	297	104	101	136
	352	103	102	138
av		102	99	134
high pressure average		109	107	147
Low Pressure Data				
10	298	115	115	130
12	298	100	100	113
13	298	79	79	90
14	298	89	89	100
this work	229	100	100	116
	263	120	120	140
	298	86	86	100
	351	89	89	104
	389	107	107	124
av		100	100	117
low pressure data		98	98	113

[a] (a) $k_0 = 2.3 \times 10^{-30}(T/298)^{-2.9}$ cm^6 s^{-1}, $k_\infty = 1.3 \times 10^{-11}(T/298)^{-2.0}$ cm^3 s^{-1}. (b) $k_0 = 2.3 \times 10^{-30}(T/298)^{-2.9}$ cm^6 s^{-1}, $k_\infty = 1.2 \times 10^{-11}(T/298)^{-1.6}$ cm^3 s^{-1}. (c) $k_0 = 2.6 \times 10^{-30}(T/300)^{-2.9}$ cm^6 s^{-1}, $k_\infty = 2.4 \times 10^{-11}(T/300)^{-1.3}$ cm^3 s^{-1}.

$k_\infty = 2.4 \times 10^{-11}(T/300)^{-1.3}$ cm^3 molecule^{-1} s^{-1}, NASA evaluation.[19] Table III shows the percentage of the experimentally determined rate constants for reaction 1 that were predicted by using these three sets of k_0 and k_∞ values, the experimental temperatures and pressures, and eq 3. Both sets of parameters (a) and (b) do about equally well at calculating the rate constants in the falloff region, giving 109 and 107%, respectively, as an average for all of the data. These do much better than (c) from the NASA evaluation,[19] which results in 147% of the experimentally determined rate constants. In the low pressure region $k = k_0[M]$ and all three expressions give good agreement with the experimental data, since there is only a small difference in the k_0 values.

The major part of the discrepancy between the results of the NASA evaluation[19] and the available experimental data for reaction 1 is in the high-pressure region, and is due to the choice of k_∞. Even if Troe's expression (3)[20,21] is not theoretically correct, the expression using the parameters (a) or (b) gives a much better empirical fit of the data for reaction 1 than does the NASA[19] choice of parameters, (c). This empirical accuracy is required for tropospheric and stratospheric modeling.

Figure 2 shows a plot of the altitude dependence of the rate constant for reaction 1 calculated by using the simplified falloff expression (3)[20,21] for standard atmosphere conditions.[23] The solid line shows the effective bimolecular rate constant with the values (b) for k_0 and k_∞, while the dashed line represents the results of a recent evaluation of data, (c).[19] The evaluation gives effective bimolecular rate constants which average about 40% higher than those determined in this work, although these results are within the range of uncertainties claimed in the evaluation.[19] The

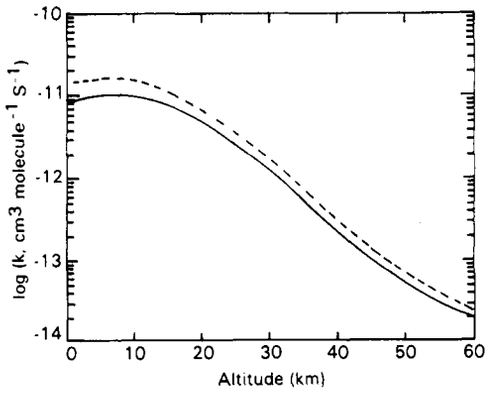

Figure 2. Plot of the altitude dependence of the effective bimolecular rate constant for reaction 1 in N_2. The solid line was calculated from eq 3 by using $k_0 = 2.3 \times 10^{-30}(T/298)^{-2.9}$ cm^6 s^{-1} and $k_\infty = 1.2 \times 10^{-11}(T/298)^{-1.6}$ cm^3 s^{-1} derived in this work, while the dashed line used $k_0 = 2.6 \times 10^{-30}(T/300)^{-2.9}$ cm^6 s^{-1} and $k_\infty = 2.4 \times 10^{-11}(T/300)^{-1.3}$ cm^3 s^{-1} from the recent evaluation.[19]

altitude dependence calculated by using k_∞ from Anastasi and Smith,[7] (a), was within about 10% of the solid line shown in Figure 2. Zellner[21] has also evaluated the rate of this reaction and has assumed a temperature independent value for k_∞. Those results[21] average about 20% higher than the results of this work.

Acknowledgment. The author gratefully acknowledges the assistance of R. D. Stephens during the course of these experiments.

Supplementary Material Available: Supplementary Tables I–VI containing kinetic data for the OH + NO_2 + M → HNO_3 + M reaction, where M is He or N_2, and over the temperature, range 229–389 K (13 pages), are available. Ordering information is given on any current masthead page.

References and Notes

(1) P. J. Crutzen, *Q. J. R. Meteorol. Soc.*, **96**, 320 (1970).
(2) R. W. Stewart, S. Hameed, and J. P. Pinto, *J. Geophys. Res.*, **82**, 3134 (1977).
(3) J. Fishman and P. J. Crutzen, *J. Geophys. Res.*, **82**, 5897 (1977).
(4) J. G. Calvert, *Environ. Sci. Technol.*, **10**, 256 (1976).
(5) C. Morley and I. W. M. Smith, *J. Chem. Soc., Faraday Trans. 2*, **68**, 1016 (1972).
(6) C. Anastasi, P. P. Bemand, and I. W. M. Smith, *Chem. Phys. Lett.*, **37**, 370 (1976).
(7) C. Anastasi and I. W. M. Smith, *J. Chem. Soc., Faraday Trans. 2*, **72**, 1459 (1976).
(8) R. Atkinson, R. A. Perry, and J. N. Pitts, Jr., *J. Chem. Phys.*, **65**, 306 (1976).
(9) P. H. Wine, N. M. Kreutter, and A. R. Ravishankara, *J. Phys. Chem.*, **83**, 3191 (1979).
(10) J. G. Anderson and F. Kaufman, *Chem. Phys. Lett.*, **16**, 375 (1972).
(11) A. A. Westenberg and N. de Haas, *J. Chem. Phys.*, **57**, 5375 (1972).
(12) J. G. Anderson, J. J. Margitan, and F. Kaufman, *J. Chem. Phys.*, **60**, 3310 (1974).
(13) C. J. Howard and K. M. Evenson, *J. Chem. Phys.*, **61**, 1943 (1974).
(14) G. W. Harris and R. P. Wayne, *J. Chem. Soc., Faraday Trans. 1*, **71**, 610 (1975).
(15) K. Erler, D. Field, R. Zellner, and I. W. M. Smith, *Ber. Bunsenges. Phys. Chem.*, **81**, 22 (1977).
(16) J. C. Polyani and J. J. Sloan, *Int. J. Chem. Kinet., Symp. 1*, 51 (1975).
(17) J. A. Silver, W. L. Dimpfl, J. H. Brophy, and J. L. Kinsey, *J. Chem. Phys.*, **65**, 1811 (1976).
(18) J. E. Spencer and G. P. Glass, *Chem. Phys.*, **15**, 35 (1976).
(19) W. B. DeMore, "Chemical Kinetic and Photochemical Data for Use in Stratospheric Modeling. Evaluation Number 2", JPL Publication 79-27, Pasadena, CA, 1979.
(20) J. Troe, *J. Phys. Chem.*, **83**, 114 (1979).
(21) R. Zellner, *Ber. Bunsenges. Phys. Chem.*, **82**, 1172 (1978).
(22) K. Glanzer and J. Troe, *Ber. Bunsenges. Phys. Chem.*, **78**, 71 (1974).
(23) National Oceanic and Atmospheric Administration, "U. S. Standard Atmosphere, 1976", Washington, D.C., 1976.